Available online at www.sciencedirect.com
ScienceDirect
C. R. Physique 7 (2006) 805–815
COMPTES RENDUS PHYSIQUE
http://france.elsevier.com/direct/COMREN/

Towards reconfigurable and cognitive communications/Vers des communications reconfigurables et cognitives

Opportunistic scheduling using cognitive radio ☆

Mischa Dohler [a,*], Seyed A. Ghorashi [b], Mohamed Ghozzi [a], Marylin Arndt [a], Fatin Said [b], A. Hamid Aghvami [b]

[a] *France Télécom R&D, 28, chemin du vieux chêne, 38243 Meylan cedex, France*
[b] *King's College London, Centre for Telecoms Research, London WC2B 5RL, UK*

Available online 7 September 2006

Abstract

Traditional cognitive approaches based on interference scanning discard a certain communication band once interference is detected, irrespective of the temporal characteristics of the interference. The aim of this article is to alert the community that interference exhibits temporal fluctuations, which can be exploited by a cognitive radio in an opportunistic manner. To this end, we present some mathematical approaches that describe the temporal behaviour of interference signals obeying a lognormal shadowing distribution. We derive some key quantities, such as throughput, for an example hierarchical cell structure configuration of a microcell hotspot being operated within a macrocell using the same frequency band. ***To cite this article: M. Dohler et al., C. R. Physique 7 (2006).***

Résumé

Ordonnanceur opportuniste à base de radio cognitive. Dans les approches cognitives traditionnelles basées sur la recherche d'interférence, une bande de communication sur laquelle est détectée de l'interférence est éliminée sans prendre en compte les caractéristiques temporelles de cette dernière. L'objectif de ce papier est d'alerter la communauté scientifique sur l'intérêt de pendre en compte les caractéristiques temporelles de l'interférence. Ainsi le terminal à radio cognitive pourra gérer de façon opportuniste l'interférence présente dans les réseaux. Dans ce but, une modélisation mathématique du comportement temporel de l'interférence est réalisée lorsque ces signaux obéissent à une loi de distribution log-normale. Dans le cas particulier d'une microcellule (hot-spots) faisant partie d'une macro cellule et communicant toutes deux sur la même bande de fréquence, des paramètres clés tel que le débit sont déterminés. ***Pour citer cet article : M. Dohler et al., C. R. Physique 7 (2006).***

Keywords: Opportunistic radio; Cognitive radio; Hierarchical cell structure; CDMA; Throughput

Mots-clés : Radio opportuniste ; Radio cognitive ; Structure hiérarchique ; CDMA ; Débit

☆ This work was partially supported by the EPSRC under grant GR/S62017/01.
* Corresponding author.
E-mail addresses: mischa.dohler@orange-ft.com (M. Dohler), seyed.ghorashi@kcl.ac.uk (S.A. Ghorashi), mohamed.ghozzi@orange-ft.com (M. Ghozzi), marylin.arndt@orange-ft.com (M. Arndt), fatin.said@kcl.ac.uk (F. Said), hamid.aghvami@kcl.ac.uk (A.H. Aghvami).

1631-0705/$ – see front matter
doi:10.1016/j.crhy.2006.07.004

1. Introduction

A cognitive radio is a device which is able to sense the communication environment and make intelligent decisions so as to enhance the overall system performance [1]. Due to an increasing density of competing wireless communication terminals and standards, cognition will play a central role in future communication systems for decreasing mutual interference and hence increasing capacity and minimising delays [1,2].

A cognitive radio consists of many components, but mainly of a sensing, decision and executive unit. In dependency of the exact realisation of these three units, a variety of different cognitive radios exist. For example, a sensing unit may be able to scan variable bandwidths at different central frequencies for interference, and the decision unit may use some neural network to draw a decision on the band to be used so as to maximise its own throughput but minimise potential interference to other systems, and the executive unit changes physical parameters within the radio chain.

Traditional cognitive approaches based on interference scanning discard a certain communication band once interference is detected, irrespective of the temporal characteristics of the interference. The aim of our paper is to alert the community that interference exhibits temporal fluctuations, which can be exploited by a cognitive radio in an opportunistic manner. To this end, we present some mathematical approaches that describe the temporal behaviour of interference signals obeying a lognormal shadowing distribution.

We will also demonstrate that only non-real time services can be supported by such a cognitive radio. However, as future personal communication systems are supposed to support a variety of services, including real-time (RT) and non-real time (NRT) circuit- and packet-switched services, the importance of efficiently accommodating NRT data traffic has increased. NRT services, such as web browsing, e-mail, fax, file transfer, etc., are delay insensitive and are able to change their transmission rates from a maximum to even zero in order to release resources for other users or other systems, or wait for better channel conditions.

We will exemplify our general analysis by investigating the possibility of offering NRT services in cognitive CDMA-based hierarchical cell structures, as depicted in Fig. 1, by means of opportunistic scheduling mechanisms, which are designed to maximise throughput in a microcell but also avoid interference with on-going RT services in a macrocell. In more details, traditionally, CDMA-based hierarchical cell structures are comprised of hot-spot microcells embedded into macrocells communicating in different frequency bands. With our novel opportunistic approach, a cognitive microcell utilises the same frequency band as the macrocell to transmit NRT data. Such an opportunistic data transmission is facilitated by the time-varying macrocell interference profile owing to mobility, fading, and power control; see Fig. 2. The main idea is that, whenever the macrocell interference falls below a given threshold, the microcell schedules data with a transmission rate dependent on the microcell signal strength and the macrocell interference level [3]. For such a hierarchical system configuration, we will prove analytically that the hence created microcell transmission window is, on average, large enough to guarantee the successful transmission of data packets.

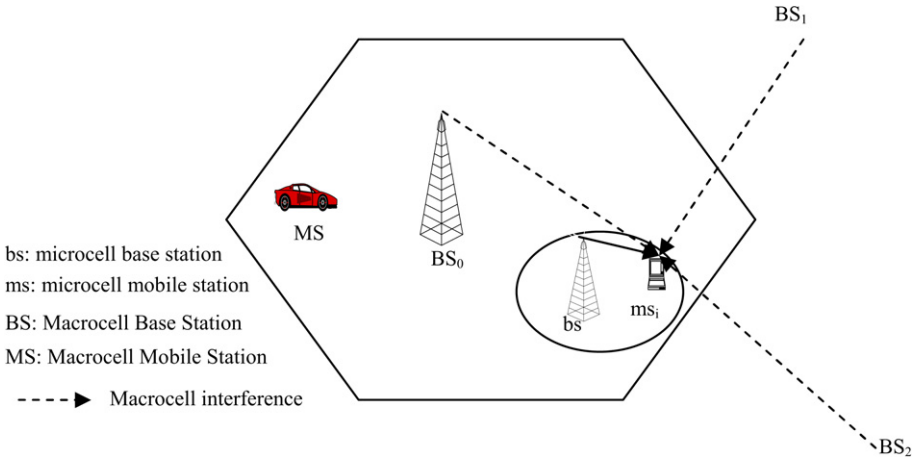

Fig. 1. Two-layer macro/microcell structure.

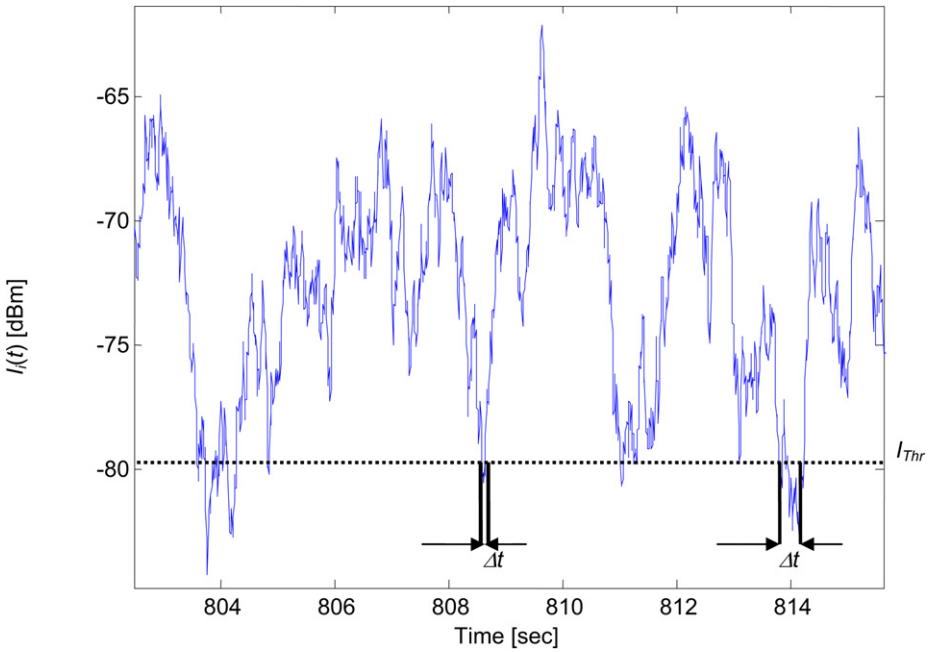

Fig. 2. A typical profile of the cross-layer interference level measured at the microcell. Data can be transmitted within the microcell at time intervals Δt, when the interference is less than a threshold (I_{Thr}).

We hence aim to demonstrate that a significant system capacity boost is feasible in opportunistic 3G and B3G cognitive communication systems; we also aim to provide an analytical framework useful for the modelling, planning and optimisation of such systems.

The paper is structured as follows. In Section 2, we present an excerpt from the state of the art related to various capacity-boosting CDMA system configurations, as well as to the analysis of time-varying channels. In Section 3, we describe the underlying system model. In Section 4, we derive the average throughput, which can be achieved by a cognitive radio requesting the data to be scheduled in an opportunistic manner. Some few simulation results are presented in Section 5. Finally, conclusions are drawn in Section 6.

2. State-of-the-art

Reviewing the coexistence of RT/NRT communications in CDMA networks mentioned in the literature, it can be found that usually the NRT data transmission is scheduled in order to adapt to the interference fluctuations and to meet the QoS requirements. In [4] the transmission of powers and rates of the NRT terminals are controlled by the network congestion level. In [5] the transmission rates of NRT terminals are controlled so that the interference of NRT terminals to RT ones remains below a given threshold. In [6] the probabilities of transmission of NRT users depend on the current or estimated state of the system. In [7] the spreading gains of NRT terminals are dynamically controlled to maximize throughput. In [8] it is shown that a time-scheduled scheme for NRT users (hybrid CDMA/TDMA) in which only one NRT user is transmitting information at any time instant, accomplishes a better throughput compared to the case that all the users are allowed to transmit information when they wish. A similar concept is proposed in [9] to support high data rate (HDR) services in the downlink of a CDMA system. In [10] a combined intracell scheduling and power control, where only one user in the cell is permitted to transmit at each instant of time is proposed. In [11], the concept of intercell scheduling or cell coordination is introduced, which is a scheduling scheme that temporarily shuts down the base stations of neighbour cells until the scheduled mobile station finishes its transmission.

Meanwhile, there are other attempts [12–16] in order to efficiently use the available bandwidth of DS-CDMA systems, i.e., the introduction of microcells within the network of macrocells where the traffic demand is high (hotspots). Although operating on a different carrier frequency eliminates cross-layer interference, sharing a carrier frequency in

both microcells and macrocells results in an increased spectral efficiency and optimisation of the available resources. However, the system has to deal with the resulting cross-layer interference.

Important for our analysis is also the prior art related to the temporal characterisation of the fading channel. Key contributions date back to [17], where average fade duration, fade outage probability for a given threshold are derived for some fading channels. However, due to interference obeying a lognormal distribution, the analysis of [18] is of great interest to us, as will become apparent in the remainder of this article.

3. System model

In this section, the system model of the cognitive radio operating in a CDMA network is introduced and the assumptions made are justified. We consider the downlink of a CDMA-based system as depicted in Fig. 1, where a microcell (mc) basestation (bs) opportunistically transmits data to a mc mobile station (ms) in the same frequency band as surrounding macrocell (MC) basestations (BS) continuously transmit data to their associated mobile stations (MS). The received signal-to-interference-plus-noise ratio ($\overline{SINR}$) of the ith user in the mc (mc serves N users) can be expressed on a linear scale as:

$$\overline{SINR}_i(t) = \frac{g_i(t)\,p_i(t)}{\sum_{j=1,\ j\neq i}^{N} \alpha_{ij}\,g_j(t)\,p_j(t) + \bar{I}(t) + \overline{N}(t)} \tag{1}$$

where $g_i(t)$ is the time-varying channel gain between the mc bs and the ith user, $p_i(t)$ is the time-varying mc bs transmission power for the ith user, α_{ij} is the code cross-correlation between user i and j as seen at the receiver (loss of code orthogonality), $\bar{I}(t)$is the total time varying MC interference, and $\overline{N}(t)$is the additive Gaussian noise.

In our case, there is clearly no code interference since the mc bs serves only one user at a time [19], i.e., $\sum_{j=1,\ j\neq i}^{N} \alpha_{ij}\,g_j(t)\,p_j(t) = 0$. Also, we assume that the micro and macro cellular CDMA systems are interference limited, i.e., we will neglect the thermal noise since in that case $\overline{N}(t) \ll \bar{I}(t)$. Furthermore, to simplify notation, we will define the signal power received by the ith user to be $\overline{S}_i(t) = g_i(t)\,P_i(t)$.

The signal power $\overline{S}_i(t)$, which is received by an L-fingered RAKE receiver, depends on the possibly power controlled transmission power, the shadowing and fading statistics. Finding an analytically tractable signal model has turned out to be impossible to date; however, assuming the shadowing process to obey a lognormal distribution and the combined fading power after RAKE reception to obey a central-χ^2 distribution with $2L$ degree of freedom [20], it can be shown that the resultant distribution is well approximated with another lognormal distribution. Furthermore, it has been demonstrated that the power control error is also likely to obey a lognormal distribution [21]. We will hence assume the received signal power at the ms to obey a lognormal distribution. The interference power $\bar{I}(t)$ is caused by the fluctuating powers coming from the surrounding MCs. It has been shown to be dominated by lognormal shadowing [22].

To simplify the notation and analysis of the occurring distributions, we will operate in the logarithmic domain, i.e., we rewrite (1) in dB as

$$SIR(t) = S(t) - I(t) \tag{2}$$

where we have neglected thermal noise and dropped the dependence on the ith user; furthermore $SIR(t) = 10\log_{10}\overline{SIR}(t)$, $S(t) = 10\log_{10}\overline{S}(t)$. In the logarithmic decibel domain, both signal and interference power obey a Gaussian distribution with given mean and variance, i.e., $S(t) \sim N(\mu_s, \sigma_s^2)$ and $I(t) \sim N(\mu_I, \sigma_I^2)$ respectively. The resultant $SIR(t)$ is therefore also Gaussian distributed with mean $\mu_s - \mu_I$ and variance $\sigma_s^2 + \sigma_I^2$, i.e., $SIR(t) \sim N(\mu_s - \mu_I, \sigma_s^2 + \sigma_I^2)$.

4. Opportunistic throughput at microcell

For a successful packet transmission from the mc bs, it is necessary that SIR not only has a value more than a given threshold, but also stays above that threshold level for at least τ_M seconds, where τ_M is the minimum time required for a packet transmission. To accommodate for this, we define the '*success event*' as the event where the $SIR(t)$ remains above a certain threshold γ_i for at least τ_M seconds. Based on this definition of a success event, we define the successful average duration of transmission, $\mathrm{ADT}_{\mathrm{Success}}$, as the average time duration that $I(t) < I_{\mathrm{Thr}}$ and

$t_e - t_s \geqslant \tau_M$, where t_s and t_e are the start and the end times of this event. We also will calculate frequency of a successful transmission, its associated probability, thereby finally facilitating the average throughput to be calculated.

In order to calculate $\mathrm{ADT}_{\mathrm{success}}$, we use the fact that for a stationary zero mean, unit variance normal process whose covariance function satisfies certain conditions specified in [23], the time interval τ that the process is above a given threshold can be modelled by a Rayleigh distributed parameter [23]. This helps to find the probability density function (pdf) of τ as well as the probability that τ is more than a given threshold, τ_M, for the zero mean and unit variance normal process of $I_n = (I - \mu_I)/\sigma_I$ as

$$f_\tau(\tau) = \frac{\lambda_I I_n^2 \tau}{4} \mathrm{e}^{-\frac{\lambda_I I_n^2 \tau^2}{8}} \tag{3}$$

and

$$P(\tau > \tau_M) = \int_{\tau_M}^{\infty} f_\tau \,\mathrm{d}\tau = \mathrm{e}^{-(\lambda_I I_n^2 \tau_M^2/8)} \tag{4}$$

The average duration of success event can now be derived as

$$\mathrm{ADT}_{\mathrm{success}} = \mathrm{e}^{A\tau_M^2}\left[\tau_M \mathrm{e}^{-A\tau_M^2} + \sqrt{\frac{\pi}{A}}\, Q\big(\sqrt{2A}\tau_M\big)\right] \tag{5}$$

where $A = \lambda I_n^2/8$. Similarly, the frequency of the success event, f_{success}, can be written as

$$f_{\mathrm{success}} = LCR \times P(\tau > \tau_M) = \frac{\sqrt{\lambda}}{2\pi} \mathrm{e}^{-A(\tau_M^2 + 4/\lambda)} \tag{6}$$

Then, the probability of success, P_{success}, is defined as the fraction of time that the mc bs can successfully transmit data packets (success event), i.e.,

$$P_{\mathrm{success}} = \lim_{t\to\infty} \big(\text{Total 'success event' time in } [0, t]\big)/t \tag{7}$$

P_{success} can be written as $P_{\mathrm{success}} = f_{\mathrm{success}} \cdot \mathrm{ADT}_{\mathrm{success}}$ according to the definitions of $\mathrm{ADT}_{\mathrm{success}}$ and f_{success} [23]. Using (5) and (6), P_{success} can finally be computed as

$$P_{\mathrm{success}} = \frac{\sqrt{\lambda}}{2\pi} \mathrm{e}^{-\frac{4A}{\lambda}} \left(\tau_M \mathrm{e}^{-A\tau_M^2} + \sqrt{\frac{\pi}{A}}\, Q\big(\sqrt{2A}\tau_M\big)\right) \tag{8}$$

For the average throughput at mc bs in this case, we require to find the

$$P\big(R(t) \geqslant R_i\big) = P\big(I(t) \leqslant I_{\mathrm{Thr},i}\big) P(\tau > \tau_M) \tag{9}$$

Then, using (4), the average throughput is given by

$$\Theta_{\mathrm{success}} = -\frac{c}{2} \mathrm{e}^{-A\tau_M^2} \mathrm{e}^{\frac{\sigma_I^2 - 2\kappa\mu_I}{2\kappa^2}} \operatorname{erf}\left(\frac{\kappa^2 Ln(c/x) - \kappa\mu_I + \sigma_I^2}{\sqrt{2}\kappa\sigma_I}\right)\Bigg|_{R_{\min}}^{R_{\max}} \tag{10}$$

where $\kappa = 10/\operatorname{Ln} 10$, $c = (W/\Gamma) g p_{\max}$, W is the bandwidth, Γ bit-energy-to-noise-spectral density ratio required to support the given service, g is the path-loss and $p_{\max}$ is the maximum transmission power at the microcell basestation. Furthermore, $R_{\max}$ and $R_{\min}$ are the maximum and minimum data rates.

5. System level simulator

A full motion or *dynamic* system level simulator for the downlink, based on the UMTS air interface specifications [24], has been developed to verify the results of this study [25]. The simulator with a time-driven simulation engine in it, recalculates mobile positions, path-losses, mobile station cell ownerships and generates call originating/clearing events and determine the E_b/I_o, at regular time intervals. Seven macrocells, including the given cell in the centre and six adjacent cells in the first tier are simulated, with a wrap around effect to keep the density of the users fixed. Based on mobility model suggested in [24], the direction of the mobile stations can be changed after the mobile station travels a minimum distance, the decorrelation length, according to a given probability. The direction change

Table 1
UMTS system level simulator parameters

Multiple access	WCDMA (FDD-Downlink)
Macrocell radius	2000 m
Microcell radius	100 m
Code orthogonality factor	0.5
Path-loss model	Okumura–Hata [22]
Chip rate	3.84 Mchips/s
Log-normal large scale fading	$\mu = 0, \sigma = 8$ dB
Max. BS power	40 dBm
Wrap around technique	Used
MS's speed	36 km/h
Max. angle of MS direction update	22.5°
Decorrelation length	20 m

is chosen randomly within $[0, \theta_{\max}]$, where $\theta_{\max}$ is the maximum angle for the direction update. The speed of mobile stations is assumed to be constant. Mobile stations are also assumed to be uniformly distributed on the cell layout and their direction is randomly chosen at initialization. A fast closed-loop power control is implemented at the BSs. The total transmit power at the BS does not exceed a maximum threshold. Also, transmission power per link must be lower than a maximum threshold set by higher layer signalling. Within the simulator, the total interfering power from all MCs is calculated as

$$\bar{I}(t) = \sum_{j=0}^{N_{\mathrm{MC}}} P_{Tx,j}(t) \cdot g_j \cdot s_j \tag{11}$$

where N_{MC} is the total number of MCs, and $j = 0$ corresponds to the closest MC. $P_{Tx,j}(t)$ is the time varying transmission power of the jth MC. g_j is the path-gain from the jth MC, and s_j is the shadowing from the jth MC in dB assumed to be an independent zero-mean Gaussian random process. To obtain the path-gain, we have utilised the corrected UMTS path-loss model [26], which, in dB, is given as

$$g_{j,\mathrm{dB}} = -87.7 + 2.4\Delta h_{b,j} - 21\log_{10}(f_c) + 18\log_{10}(\Delta h_{b,j}) - 40 \cdot [1 - 2 \times 10^{-2}\Delta h_{b,j}] \cdot \log_{10}(x_j) \tag{12}$$

where $\Delta h_{b,j}$ in [m] is the jth MC BS antenna height measured from above the roof level, f_c in [MHz] is the operational communication frequency, and x_j in [km] is the distance from the jth MC BS.

A mc location-dependent MC-to-mc interference sequence is generated as the output of the dynamic simulator, which facilitates the analysis of the data transmission analysis within the mc. The simulator has been benchmarked and successfully utilised in a variety of studies [25,27,28]. The main simulation parameters are summarised in Table 1 for the sake of clarity.

6. Numerical results

The mc average throughput as a function of the average of the MC interference level $I_I(t)$ is depicted in Fig. 3, where the interference is modelled by a Gaussian process, and it is compared to the throughput computed in the simulation. The set of feasible data rates for the simulation is $\vec{R} = \{0, 8, 16, 32, 64, 128, 256, 512, 1024, 2048, 4096\}$ [kbps]. For $\Gamma_i = 3$ dB [8], $W = 3.84$ MHz, $P_{\max} = 30$ dBm, $g_i = -110$ dB [13], the set of I_{Thr} can be written as $I_{\mathrm{Thr}} = \{\infty, -56.2, -59.2, -62.2, -65.2, -68.2, -71.2, -74.2, -77.2, -80.2, -83.2, -\infty\}$ [dBm]. The curve shows that when the MC interference average, μ_I, is less than -90 dBm, data transmission with the maximum possible data rate (4096 kbps) is possible. On the other hand, it can be seen that even when the interference mean μ_I is 40 dB larger ($\mu_I = -50$ dBm), a throughput of 1 kbps is still possible, which can be used for some services in microcell.

The impact of τ_M on the average throughput for Gaussian process and simulation results is presented in Fig. 4; as the minimum required time interval of the packet transmission increases, the average throughput decreases. Notice that the slope of the curve at the time intervals of < 1 s, in which most of possible packet lengths are, is higher. This shows the high sensitivity of the throughput at mc bs to the minimum packet length (or the minimum time needed for transmission of a packet).

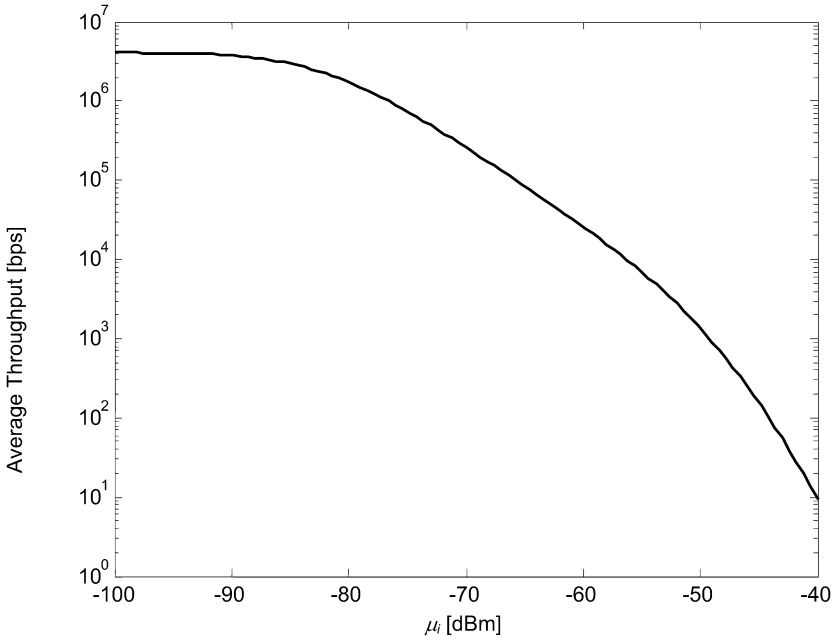

Fig. 3. Average throughput at the microcell as a function of average interference, μ_i, assuming that: $\Gamma_i = 3$ dB, $W = 3.84$ MHz, $P_{\max} = 30$ dBm, $g_i = -110$ dB, and $R = \{0, 8, 16, 32, 64, 128, 256, 512, 1024, 2048, 4096\}$ [kbps].

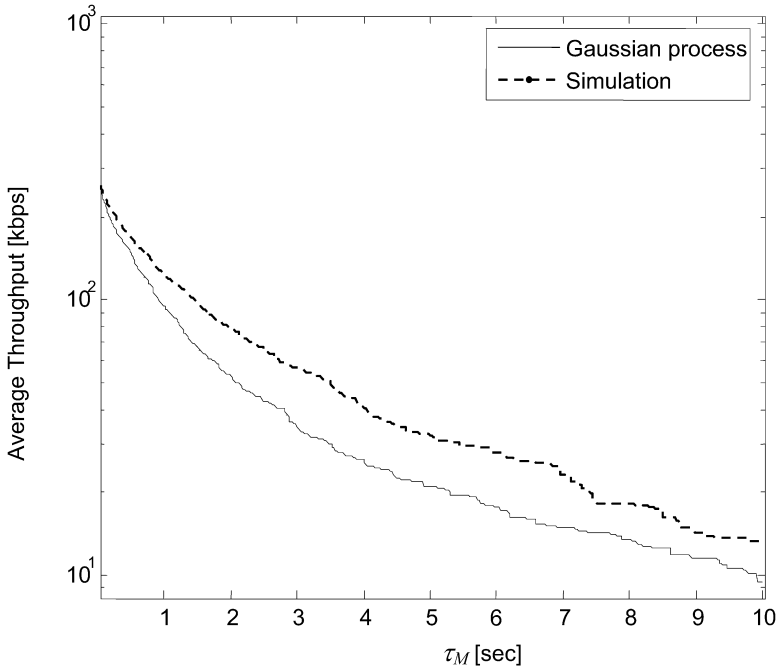

Fig. 4. Average throughput at the microcell as a function of τ_M, assuming: $\mu_I = -70$ dBm, $\sigma_I = 5.43$ dBm, $\Gamma_i = 3$ dB, $W = 3.84$ MHz, $P_{\max} = 30$ dBm, $g_i = -110$ dB, and $R = \{0, 8, 16, 32, 64, 128, 256, 512, 1024, 2048, 4096\}$ [kbps].

While the impact of MC interference average, μ_I, on the data transmission at mc bc is predictable, the effect of the standard deviation, σ_I, is not that trivial. However, for the sake of brevity, this has been omitted here. Finally, it can also be seen from Fig. 5 that the slope of the average throughput changes as a function of τ_M, i.e., it decreases with decreasing σ_I. This means that interference profiles with higher standard deviations are more sensitive to the packet

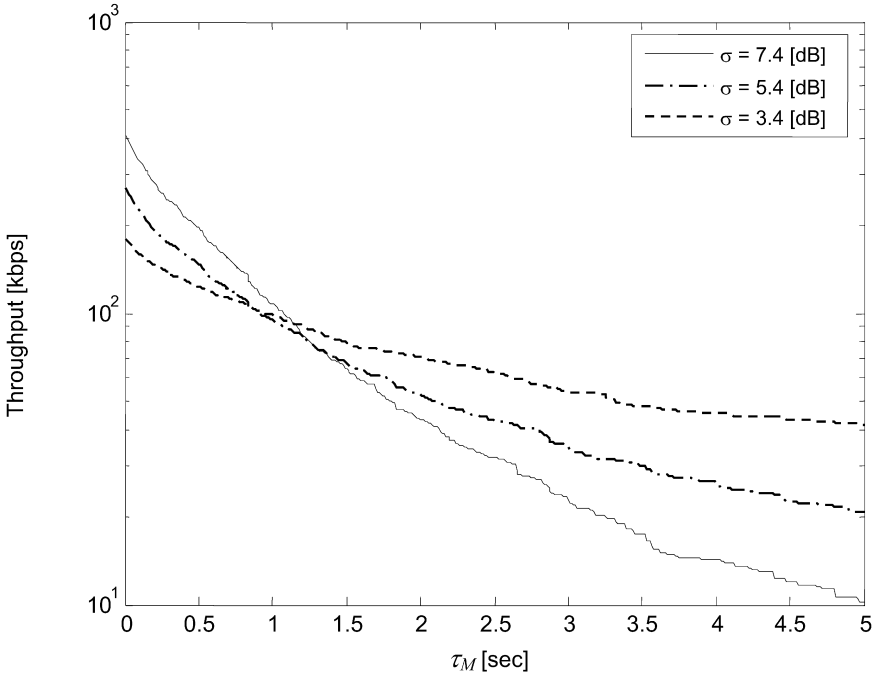

Fig. 5. Throughput at the microcell as a function of τ_M for different σ_I, assuming: $\mu_I = -70$ dBm, $\Gamma_i = 3$ dB, $W = 3.84$ MHz, $P_{\max} = 30$ dBm, $g_i = -110$ dB, and $R = \{0, 8, 16, 32, 64, 128, 256, 512, 1024, 2048, 4096\}$ [kbps].

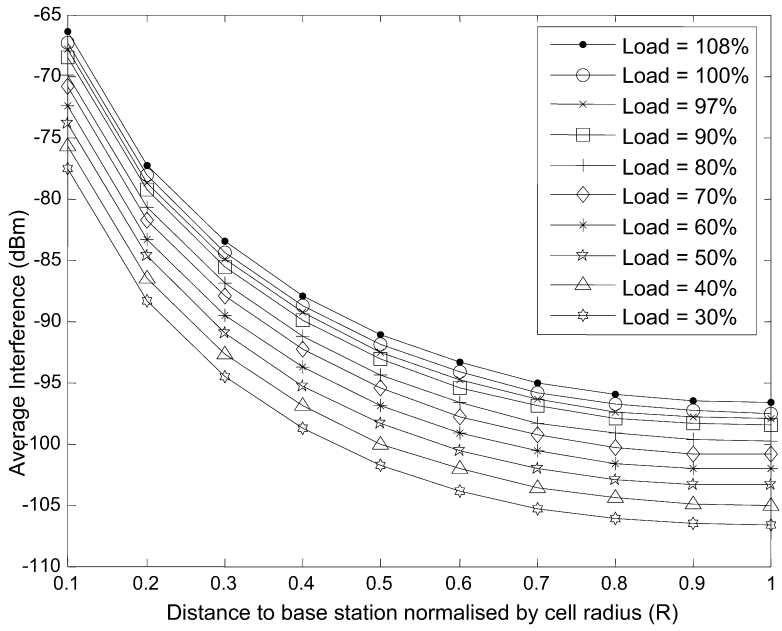

Fig. 6. Average interference as a function of microcell mobile station distance to macrocell base station, for different macrocell loads (voice users).

length, which is a useful insight into the design of optimum packet lengths in dependency of the fading channel identified by the cognitive radio.

As just mentioned, the mean interference value of the MC interference, μ_I, as well as the standard deviation of $I(t)$, σ_I, have a major impact on the achievable throughput of the mc bs. Given their importance, we monitored by means of the system level simulator the experienced interference statistics in a cellular systems for different positions

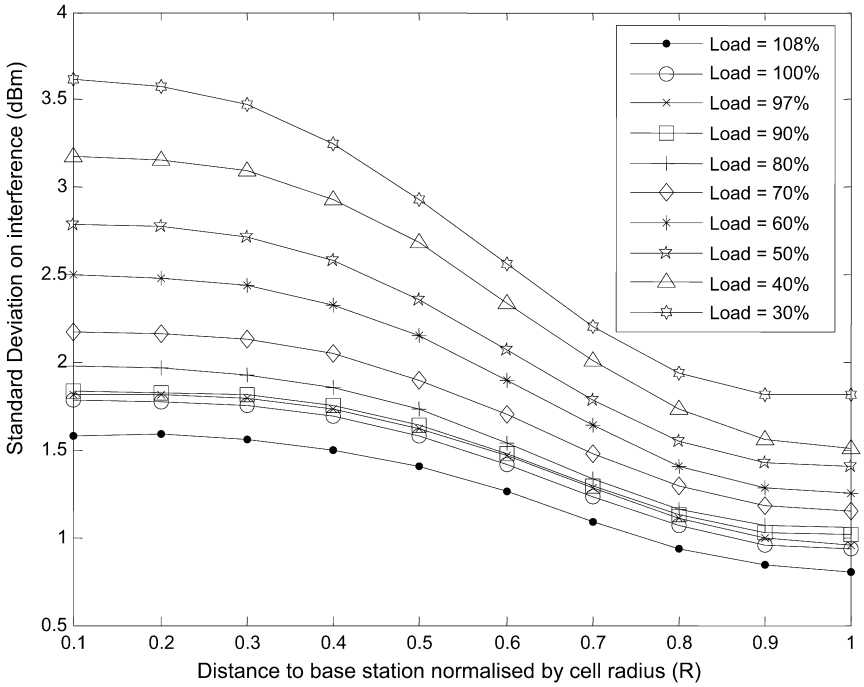

Fig. 7. Standard deviation of interference as a function of microcell mobile station distance to macrocell base station, for different macrocell loads (voice users).

of the mc bs and different load percentages of the MC, where a 100% load is defined for a given number of users having a blocking probability of 2%. The results are depicted in Figs. 6 and 7. Fig. 6 illustrates μ_I as a function of the target mc receiver distance to the central MC base station in a network of hexagonal cells, for voice users. It can be seen that by varying the load from 30% to 100%, μ_I changes around 10 dB within the whole area of the MC. Looking at the variations of σ_I in Fig. 7, we find out that at low traffic conditions (load $< 70\%$), σ_I decreases rapidly for an increasing distance to the MC BS. This is because in the close neighborhood of the serving BS, the interference comes from the dominant BS, but going to the borders of the cell, the interference is a combination of several components coming from different BSs. The variation of σ_I is less for high traffic conditions; σ_I is almost constant for the cases that the load is larger than 70%. This is due to the saturation of transmit power for high number of MSs in the cell. Figs. 6 and 7 show that although going to the centre of the cell increases the mean interference level, which definitely causes a decrease in achievable throughput at the mc, but at the same time the standard deviation of the interference increases and this counteracts the throughput reduction.

Finally, Fig. 8 illustrates the achievable throughput at the mc bs as a function of the standard deviation of interference for different μ_I, for the case of a discrete set of feasible date rates. In both cases, we can see that the throughput increases by increasing σ_I; however, the throughput saturates because the maximum data rate is limited. Comparing these results with those of Figs. 6 and 7 shows how the location of a mc bs in the MC and also the load of the MC can affect the achievable throughput at the microcell.

7. Conclusions

We have introduced and analysed a novel approach for a cognitive radio organising data scheduling within CDMA-based hierarchical cell structures with the microcell and macrocell utilising the same frequency band. Although we have not analysed, in fact neglected, the effect of the interference created by the microcell onto the macrocell, it is apparent that such cognitive approach facilitates the system capacity to be increased.

We have proposed to serve real-time services within the umbrella macrocell, whereas non-real time traffic is opportunistically offered within the microcell. Such opportunistic data transmission, as analytically corroborated in this paper, is facilitated by the time varying macrocell interference profile owing to mobility, fading, and power control.

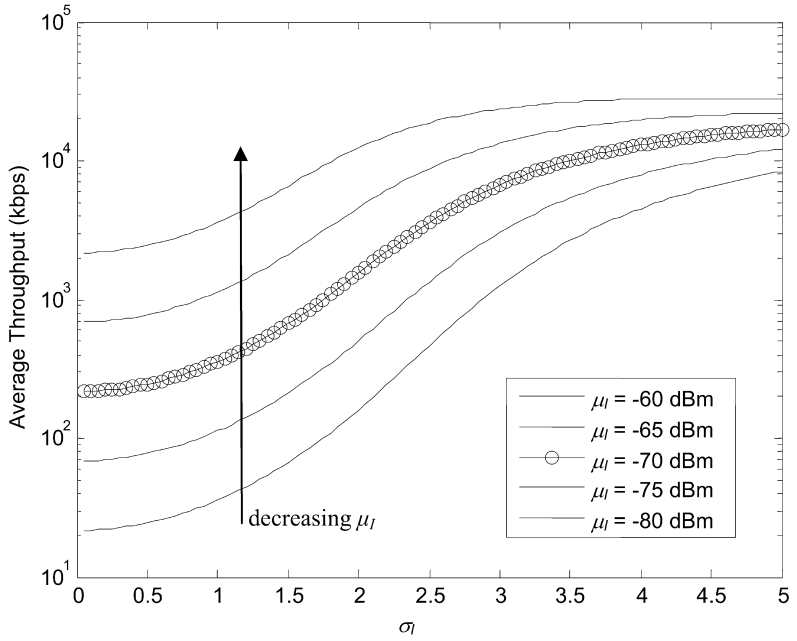

Fig. 8. Average throughput as a function of macrocell interference standard deviation, σ_I, for different mean interference levels, μ_I, for the case of discrete feasible date rates.

We have demonstrated that the macrocell interference falls below a given threshold for a sufficient time period, thereby allowing the microcell to schedule data with a transmission rate dependent on the microcell signal strength and macrocell interference level. We have hence derived the average duration, the frequency of transmission and probability of successful transmission for non-real time data transmission.

The derived performance metrics have been verified by means of an UMTS system level simulator, which incorporates several tiers of interfering macrocells, mobility, power control, shadowing, etc. A large variety of studies has confirmed the correctness of the system assumptions as well as the performed analysis.

Despite giving clear deployment guideline, the analysis facilitates an analytical optimisation and treatment of scheduling protocols within cognitive CDMA-based systems, possibly in conjunction with heterogeneous deployments, without the need for lengthy and complex system level simulations.

References

[1] S. Haykin, Cognitive radio: Brain-empowered wireless communications, IEEE J. Select. Areas Commun. 23 (2) (February 2005) 201–220.
[2] J. Mitola, et al., Cognitive radio: Making software radios more personal, IEEE Pers. Commun. 6 (4) (August 1999) 13–18.
[3] S.A. Ghorashi, H.K. Cheung, F. Said, A.H. Aghvami, Performance of a CDMA based HCS network with hybrid speed/overflow sensitive handover strategy, IEE Proc. Commun. 150 (4) (August 2003) 293–297.
[4] J.M. Jacobsmeyer, Congestion relief on power-controlled CDMA networks, IEEE J. Select. Areas Commun. 14 (December 1996) 1758–1761.
[5] J.M. Capone, L.F. Merakos, Integrating data traffic into a CDMA cellular voice system, ACM Wireless Networks 1 (4) (1995) 389–402.
[6] C.-L. I, K.K. Sabnani, Variable spreading gain CDMA with adaptive control for true packet switching wireless network, in: Proc. IEEE ICC, Seattle, WA, 1995, pp. 1060–1064.
[7] Seong-Jun Oh, K.M. Wasserman, Dynamic spreading gain control in multiservice CDMA networks, IEEE J. Select. Areas Commun. 17 (5) (May 1999) 918–927.
[8] S. Ramakrishna, J.M. Holtsman, A scheme for throughout maximization in a dual-class CDMA system, IEEE J. Select. Areas Commun. 16 (August 1998) 830–844.
[9] P. Bender, P. Black, M. Grob, R. Padovani, N. Sindhushyana, A. Viterbi, CDMA/HDR: A bandwidth-efficient high-speed wireless data service for nomadic users, IEEE Commun. Mag. 38 (2000) 70–77.
[10] F. Berggren, S.-L. Kim, R. Jantti, J. Zander, Joint power control and intracell scheduling of DS-CDMA non-real time data, IEEE J. Select. Areas Commun. 19 (2001) 1860–1870.
[11] Sung-hyuk Kwon, Seong-Lyun Kim, R. Jantti, Downlink intercell coordination for DS-CDMA non-real time data, in: IEEE Veh. Tech. Conf. (VTC 2003-Spring), vol. 3, April 2003, pp. 1689–1693.

[12] Dong Hee Kim, Dong Do Lee, Ho Joon Kim, Keum Chan Whang, Capacity analysis of macro/microcellular CDMA with power ratio control and tilted antenna, IEEE Trans. Veh. Technol. 49 (1) (January 2000) 34–42.
[13] Jung-Shyr Wu, Jen-Kung Chung, Yu-Chuan Yang, Performance study for a microcell hot-spot embedded in CDMA macrocell systems, IEEE Trans. Veh. Technol. 48 (1) (January 1999) 47–59.
[14] Cheolin Joh, Keunyoung Kim, Youngnam Han, Performance of a microcell with optimal power allocation for multiple class traffic in hierarchically structured cellular CDMA systems, in: IEEE Veh. Tech. Conf. (VTC 2001-Spring), 2001, pp. 2818–2822.
[15] S. Hamalainen, H. Lilja, J. Lokio, M. Leinonen, Performance of a CDMA based hierarchical cell structure network, in: 8th IEEE International Symposium on Personal, Indoor and Mobile Radio Communications (PIMRC 97), vol. 3, 1997, pp. 863–866.
[16] A. Catovic, S. Tekinay, Projection multiuser detectors for hierarchical cell structures in CDMA cellular systems, in: IEEE Veh. Tech. Conf. (VTC 2001-Spring), vol. 3, 2001, pp. 1853–1857.
[17] W.C.Y. Lee, Mobile Communications Engineering, McGraw-Hill, New York, 1982 (Chapter 3).
[18] N.B. Mandayam, P. Chen, J.M. Holtzman, Minimum duration outage for cellular systems: A level crossing analysis, in: Proc. IEEE VTC, April 1996, pp. 879–883.
[19] R. Steele, L. Hanzo, Mobile Radio Communications, second ed., May 1999.
[20] M.K. Simon, M.-S. Alouini, Digital Communication over Fading Channels, John Wiley & Sons, Inc., New York, 2000.
[21] A.J. Viterbi, CDMA: Principles of Spread Spectrum Communications, second ed., Addison–Wesley, 1992.
[22] L. Wang, A.H. Aghvami, W.G. Chambers, Capacity estimation of SIR-based power controlled CDMA cellular systems in presence of power control error, IEICE Trans. Commun. E86-B (9) (September 2003).
[23] R. Vijayan, J.M. Holtzman, Foundations for level crossing analysis of handoff algorithms, in: ICC 93, vol. 2, May 1993, pp. 935–939.
[24] ETSI: Universal Mobile Telecom. System (UMTS); Selection procedures for the choice of radio transmission of UMTS, UMTS technical report 30.03, v. 3.2.0, April 1998.
[25] S.A. Ghorashi, E. Homayounvala, F. Said, A.H. Aghvami, Dynamic simulator for studying WCDMA based hierarchical cell structures, in: PIMRC 2001, vol. 1, September 2001, pp. 32–37.
[26] J.M. Hernando, L. Mendo, Corrections to the path loss model for UMTS vehicular test environment, IEEE Trans. Veh. Technol. 50 (1) (January 2001) 331.
[27] S.A. Ghorashi, H.K. Cheung, F. Said, A.H. Aghvami, Performance of a CDMA based HCS network with hybrid speed/overflow sensitive handover strategy, IEE Proc. Commun. 150 (4) (August 2003) 293–297.
[28] S.A. Ghorashi, F. Said, A.H. Aghvami, Handover rate control in hierarchically structured cellular CDMA systems, in: PIMRC 2003, vol. 3, September 2003, pp. 2083–2087.